Supporting Material for publication

Graphene/Ru(0001)

As a consequence of the existence of ripples in monolayer graphene (MLG) on Ru(0001) [1, 2], the LEED pattern shows satellite spots caused by the moiré structure (Figure S1).

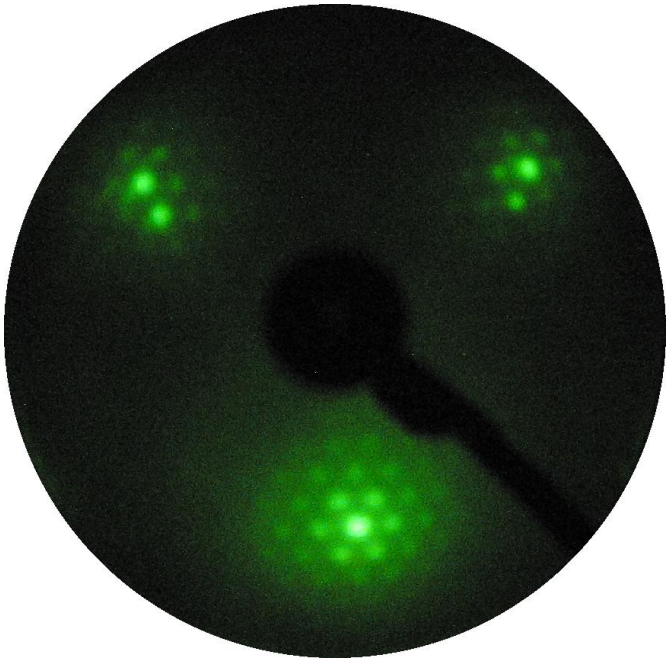

Figure S1: LEED pattern of graphene on Ru(0001), recorded at Ep = 74 eV and at room temperature.

Further characterization of the MLG has been carried out by the measurement of phonon modes [3-6] (Figure S2). The presence of well-resolved ZA (out-of-plane acoustic), TA (transverse acoustic), LA (longitudinal acoustic), and LO (longitudinal optical) phonons ensures of the good order and crystalline quality of the graphene sheet. Similar results have been attained for MLG/Pt(111), as already reported in our previous works [4, 5, 7].

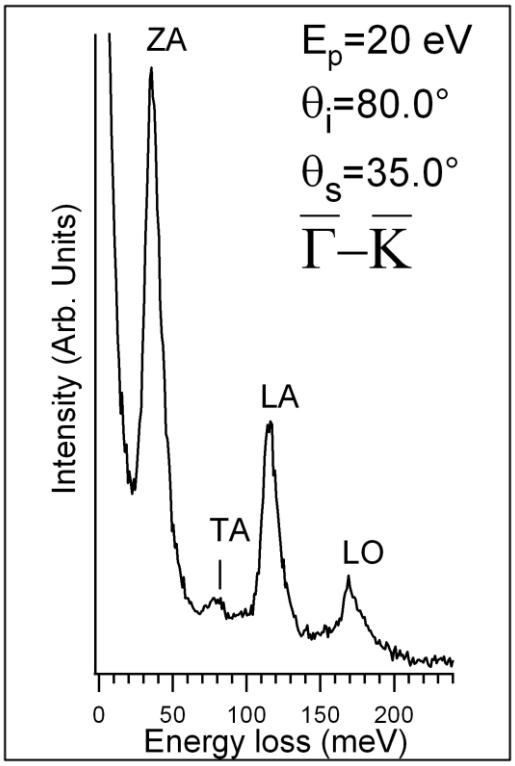

Figure S2: HREEL spectrum of the MLG/Ru(0001) for an impinging energy of 20 eV. The incidence angle is 80.0° while the scattering angle is 35.0°. The sample was oriented along the $\overline{\Gamma}-\overline{K}$ *direction.*

As concerns the microscopic investigation of air-exposed graphene/Ru(0001), the reader is referred to the previous complete study in Ref. [2] by Politano et al.

Graphene/Pt(111)

LEED

The graphene growth on Pt(111) substrate was monitored in-situ by LEED spectroscopy. This analysis suggests that the saturation of a monolayer graphene (MLG) on the Pt (111) substrate was reached upon an exposure of ethylene of $3 \cdot 10^{-8}$ mbar for ten minutes (24 Langmuir). As demonstrated also by in-situ low-energy electron microscopy studies [8], no nucleation and growth of additional graphene sheets beyond the MLG occurs on Pt(111) [8-15].

The presence of well-resolved spots in the LEED pattern (see Figure S3) is a clear fingerprint of the order of the MLG over-structure. The attained LEED pattern is essentially similar to that reported by Gao et al. [10]. The ring pattern indicates the existence of different domains. Nonetheless, preferred orientations aligned with the substrate (R0) are clearly distinguished.

Despite the presence of other domains, the predominance of R0 domains has been clearly inferred by the analysis of phonon dispersion measurements by Politano et al. reported in Ref. [4].

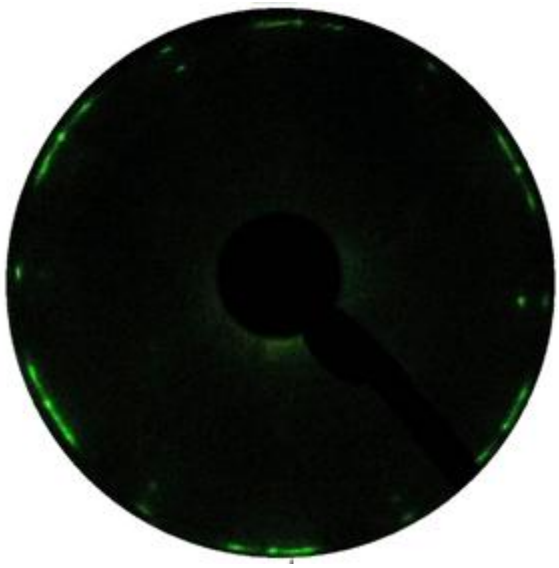

Figure S3: LEED pattern of graphene on Pt(11), recorded at Ep = 74 eV and at room temperature.

SEM investigation on the air-exposed sample

The as-deposited graphene layer was later characterized ex-situ by SEM and micro-Raman spectroscopy, as shown more extensively in an addressed previous publication [16]. The surface morphology appears to SEM exploration homogeneous across all the sample (1x1 cm^2). SEM images (see Figure S5) show a full coverage of the substrate surface by the graphene which forms a network of wrinkles (darker horizontal and vertical lines in Figure

S5). The wrinkles network develops on a micrometric length scale. Its morphology matches that obtained by low-energy electron microscopy (LEEM) measurements for graphene grown on Pt (111) by carbon segregation from the Pt (111) substrate and other metallic substrates [8]. In addition, zones of average micrometric size, showing two different shades, are observed on the surface, probably due to different graphene domains orientations. Their presence could also be correlated to wrinkles network. Another observed detail concerns the growth of randomly distributed sub-micrometric islands, suggesting the formation of thicker graphitic structures.

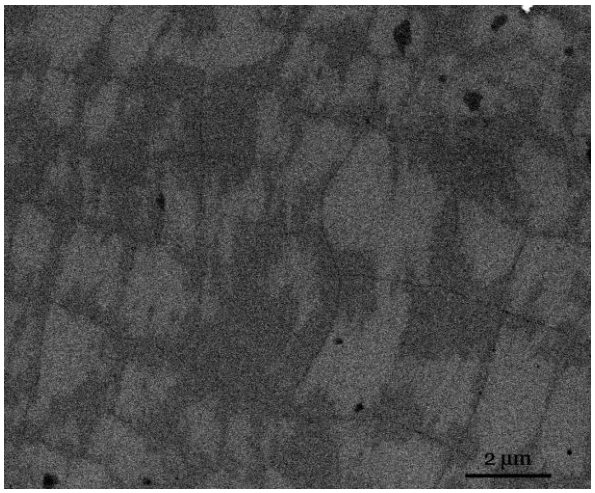

Figure S5*: Graphene layer on a Pt(111) substrate. A wrinkle network is observed (darker lines) and two main different surface shades. Note also the few small black spots randomly distributed.*

1 B. Borca, S. Barja, M. Garnica, M. Minniti, A. Politano, J. M. Rodriguez-García, J. J. Hinarejos, D. Farías, A. L. Vázquez de Parga and R. Miranda, *New J. Phys.*, 2010, **12**, 093018.
2 A. Politano, B. Borca, M. Minniti, J. J. Hinarejos, A. L. Vázquez de Parga, D. Farías and R. Miranda, *Phys. Rev. B*, 2011, **84**, 035450.
3 L. J. Karssemeijer and A. Fasolino, *Surf. Sci.*, 2011, **605**, 1611-1615.
4 A. Politano, A. R. Marino, D. Campi, D. Farías, R. Miranda and G. Chiarello, *Carbon*, 2012, **50**, 4903–4910.
5 A. Politano, A. R. Marino and G. Chiarello, *J. Phys.: Condens. Matter*, 2012, **24**, 104025.

6 G. Benedek, F. Hofmann, P. Ruggerone, G. Onida and L. Miglio, *Surf. Sci. Rep.*, 1994, **20**, 3-43.
7 A. Politano, A. R. Marino, V. Formoso and G. Chiarello, *Carbon*, 2012, **50**, 734-736.
8 P. Sutter, J. T. Sadowski and E. Sutter, *Phys. Rev. B*, 2009, **80**, 245411.
9 T. Fujita, W. Kobayashi and C. Oshima, *Surf. Interface Anal.*, 2005, **37**, 120-123.
10 M. Gao, Y. Pan, L. Huang, H. Hu, L. Z. Zhang, H. M. Guo, S. X. Du and H. J. Gao, *Appl. Phys. Lett.*, 2011, **98**, 033101.
11 B. J. Kang, J. H. Mun, C. Y. Hwang and B. J. Cho, *J. Appl. Phys.*, 2009, **106**, 104309.
12 G. Otero, C. Gonzalez, A. L. Pinardi, P. Merino, S. Gardonio, S. Lizzit, M. Blanco-Rey, K. Van de Ruit, C. F. J. Flipse, J. Méndez, P. L. de Andrés and J. A. Martín-Gago, *Phys. Rev. Lett.*, 2010, **105**, 216102.
13 A. Politano, A. R. Marino, V. Formoso, D. Farías, R. Miranda and G. Chiarello, *Phys. Rev. B*, 2011, **84**, 033401.
14 N. A. Vinogradov, K. Schulte, M. L. Ng, A. Mikkelsen, E. Lundgren, N. Mårtensson and A. B. Preobrajenski, *J. Phys. Chem. C*, 2011, **115**, 9568–9577.
15 Y. Yamada, C. Sugawara, Y. Satake, Y. Yokoyama, R. Okada, T. Nakayama, M. Sasaki, T. Kondo, J. Oh, J. Nakamura and W. W. Hayes, *J. Phys.: Condens. Matter*, 2010, **22**, 304010.
16 E. Cazzanelli, T. Caruso, M. Castriota, A. R. Marino, A. Politano, G. Chiarello, M. Giarola and G. Mariotto, *J. Raman Spectrosc.*, 2013, doi:10.1002/jrs.4285.